

## Matrix-isolation Studies on Group 3 Trihalides. Part I. Vibrational Spectra and Molecular Shapes of Monomeric Trichlorides of Aluminium, Gallium, and Indium

By Ian R. Beattie, H. Edwin Blayden, Stephen M. Hall, Simon N. Jenny, and J. Steven Ogden,\*  
Department of Chemistry, The University, Southampton SO9 5NH

High-resolution Raman and i.r. studies have been made on monomeric  $\text{AlCl}_3$ ,  $\text{GaCl}_3$ , and  $\text{InCl}_3$  isolated in argon matrices at low temperatures. All the in-plane fundamentals of these molecules are located, and it is shown that the isotope frequency and intensity patterns observed under high resolution may be interpreted using a relatively simple model which appears to have wide application. On the basis of these experiments, planar geometries are derived for all three molecules, and it is conclusively demonstrated that an earlier matrix-isolation study of  $\text{AlCl}_3$  is based on incorrect band assignments.

THERE is considerable current interest in the geometry of simple molecules at high temperatures,<sup>1</sup> and in recent years it has become clear that the information available from electric-deflection and matrix-isolation studies has posed some interesting problems for theoretical chemists. It has been found, for example, that whereas the triatomic species  $\text{BeX}_2$  ( $\text{X} = \text{halogen}$ ) all appear to be linear, the corresponding barium halides are all bent, as are the fluorides of calcium and strontium. These observations, although capable of rationalisation, were totally unexpected, and it is therefore important not only to widen our theoretical approach to such problems but also to extend experimental observations.

One obvious extension is to investigate whether the monomeric trihalides of the heavier Group 3 elements show the  $D_{3h}$  geometries found for  $\text{BX}_3$ , or, alternatively, adopt pyramidal  $C_{3v}$  structures, and this paper reports the results of an i.r. and Raman study on matrix-isolated  $\text{AlCl}_3$ ,  $\text{GaCl}_3$ , and  $\text{InCl}_3$ . When this work was undertaken, no i.r. or structural data were available for monomeric  $\text{GaCl}_3$  or  $\text{InCl}_3$ , and the position regarding  $\text{AlCl}_3$  was confusing. A previous matrix-isolation study

by Lesiecki and Shirk<sup>2</sup> suggested that  $\text{AlCl}_3$  was pyramidal with a  $\text{Cl-Al-Cl}$  angle of *ca.*  $112^\circ$ , and this conflicted with an earlier electron-diffraction study by Zasorin and Rambidi<sup>3</sup> which favoured  $D_{3h}$  symmetry.

In an earlier letter<sup>4</sup> we presented preliminary results and qualitative arguments indicating why we believe Lesiecki and Shirk's conclusions to be incorrect. This paper describes in detail our matrix-isolation studies on monomeric  $\text{AlCl}_3$ ,  $\text{GaCl}_3$ , and  $\text{InCl}_3$ , and sets out fully our reasons for preferring a  $D_{3h}$  structure for all these species. During the course of this work, we became interested in the chlorine-isotope patterns observed for these molecules under high resolution, and in the Appendix we describe not only why these patterns arise but also how they may be used quite generally to characterise molecular vibrations.

### EXPERIMENTAL

The matrix-isolation i.r. and Raman studies described in this paper were carried out using two independent 'Displex' units (Air Products, CS 202) which were incorporated in conventional high-vacuum systems operating at less than  $10^{-7}$  Torr.<sup>†</sup> The basic design for matrix-isolation i.r. and

<sup>†</sup> 1 Torr = (101 325/760) Pa, 1 dyn =  $10^{-5}$  N.

<sup>1</sup> J. W. Hastie, R. H. Hauge, and J. L. Margrave, *Ann. Rev. Phys. Chem.*, 1970, **21**, 475.

<sup>2</sup> M. L. Lesiecki and J. S. Shirk, *J. Chem. Phys.*, 1972, **56**, 4171.

<sup>3</sup> E. Z. Zasorin and N. G. Rambidi, *Zhur. strukt. Khim.*, 1967, **8**, 391.

<sup>4</sup> I. R. Beattie, H. E. Blayden, and J. S. Ogden, *J. Chem. Phys.*, 1976, in the press.

Raman experiments is by now reasonably familiar,<sup>5</sup> but it is perhaps relevant to describe one or two refinements which we found convenient for this work in connection with the design of superheaters suitable for cracking  $\text{Al}_2\text{Cl}_6$  and  $\text{Ga}_2\text{Cl}_6$ . Two models were satisfactory and are shown in Figure 1.

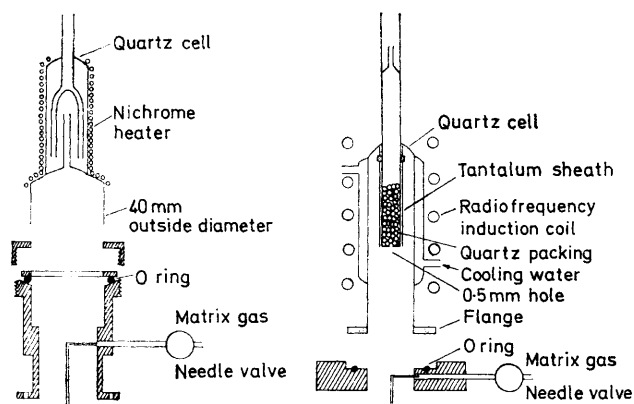


FIGURE 1 Superheater designs suitable for cracking  $\text{Al}_2\text{Cl}_6$  and  $\text{Ga}_2\text{Cl}_6$

The first model employs external resistive heating of an all-silica cell, whilst the second uses induction heating of a lightly packed silica tube *via* a cylindrical platinum or tantalum sleeve. The principal problem which these designs appear to overcome is first that cracking of  $\text{Al}_2\text{Cl}_6$  seems to be kinetically rather slow, but at elevated temperatures it appears to react readily with silica to produce  $\text{SiCl}_4$ . This potential impurity was not observed in these experiments, but has been shown<sup>6</sup> to be responsible for an unassigned band (at  $420\text{ cm}^{-1}$ ) in the original Raman studies<sup>7</sup> on  $\text{AlCl}_3$  in the vapour phase. The flow of dimer species into these superheaters was controlled by a polytetrafluoroethylene needle valve and monitored by a faint Tesla discharge. On leaving the superheater, the high-temperature vapour was mixed with a large excess of argon as shown and deposited on a cool (*ca.* 12 K) surface after traversing a path of *ca.* 40 mm. For Raman studies, a platinum mirror soldered to a high-purity copper block was a satisfactory deposition surface, whilst in the i.r. experiments conventional caesium iodide optics were employed. Cryogenic temperatures were monitored using a chromel-gold (0.3% Fe) thermocouple, and superheater temperatures were measured using an optical pyrometer or chromel-alumel thermocouple.

Matrix gas flows were typically *ca.* 5–10 mmol  $\text{h}^{-1}$ , and the amounts condensing on the cold surface could be estimated using a standard film-thickness monitor. The matrix ratios for these experiments were not measured to a high degree of accuracy, but consideration of the absorption coefficients of the more prominent i.r. fundamentals of  $\text{Ga}_2\text{Cl}_6$  indicates that they were in the range 500:1–2 000:1. Deposition times of up to 60 min were quite adequate for both i.r. and Raman studies. High-purity argon matrix gas was obtained from B.O.C. and used without further purification, whilst samples of anhydrous aluminium and gallium trichloride were prepared by direct combination, and purified by vacuum sublimation. Indium, boron, and phosphorus trichlorides were all obtained commercially and

similarly purified before use. I.r. spectra were obtained using a Perkin-Elmer 225 spectrophotometer, whilst Raman spectra were recorded on a Cary 82 instrument using argon-ion (5 145 Å) laser excitation (CRL 52B). Precise optimisation in these laser-Raman matrix studies was achieved using micrometer adjusters, and power levels were typically in the range 100–400 mW.

## RESULTS AND DISCUSSION

**Aluminium Trichloride.**—Over 20 matrix experiments were made on aluminium trichloride vapour, but of these only eight need be considered in any detail. As indicated in the Experimental section, the deposition conditions for Raman and i.r. studies were similar, and it is convenient to discuss both sets of results together.

Figure 2(a) shows the Raman spectrum obtained after condensing aluminium trichloride vapour with a large excess of argon at 12 K. In this experiment, no attempt was made to superheat the vapour, and both the sample and the superheater were maintained at *ca.* 350 K. The spectrum consists of features at 613, 523, 342, 283, 219, 166, 122, 107, 77, and  $65\text{ cm}^{-1}$ . Apart from the lowest-frequency band, which corresponds to a lattice mode of argon,<sup>8</sup> these features may all be attributed to molecular  $\text{Al}_2\text{Cl}_6$  by comparison with earlier Raman data.<sup>7</sup> Figure 2(b) shows the i.r. spectrum of a similar deposit, in which the vapourising temperature was 350 K and the four prominent bands at 620, 482, 421, and  $320\text{ cm}^{-1}$  are similarly assigned to  $\text{Al}_2\text{Cl}_6$ . These wavenumbers are similar to those obtained by Lesiecki and Shirk<sup>2</sup> (see Table 1), but the spectrum differs in one important

TABLE I  
Vibrational spectra ( $\text{cm}^{-1}$ ) and band assignments for molecular  $\text{Al}_2\text{Cl}_6$  and  $\text{Ga}_2\text{Cl}_6$

$\text{Al}_2\text{Cl}_6$			$\text{Ga}_2\text{Cl}_6$		
Ar matrix (this work)	Ar matrix (ref. 2)	Vapour (refs. 7 and 10)	Ar matrix (this work)	Vapour (refs. 7 and 15)	Assignment and activity
523		510	416	416	$\nu_1 A_g$ Raman
342		336	322	310	$\nu_2 A_g$ Raman
219		217	167	168	$\nu_3 A_g$ Raman
107		99	100	89	$\nu_4 A_g$ Raman
166		165			$\nu_7 B_{1g}$ Raman
620	620	625	468	477	$\nu_8 B_{1u}$ i.r.
613		612	467	472	$\nu_{11} B_{2g}$ Raman
122		117	115	113	$\nu_{12} B_{2g}$ Raman
421	418	420	311	310	$\nu_{13} B_{2u}$ i.r.
482	480	484	399	400	$\nu_{16} B_{3u}$ i.r.
320	320		281	280	$\nu_{17} B_{3u}$ i.r.
283		(282) *	239	(231) *	} (Not assigned)
			345	344	
77		77	77		

\* Observed in the melt.<sup>12</sup>

respect: we find that the most intense band is at  $482\text{ cm}^{-1}$ , whereas it would appear from Lesiecki and Shirk's paper that their most intense band is the feature at *ca.*  $620\text{ cm}^{-1}$ . Both the bands at 620 and  $482\text{ cm}^{-1}$  show partially resolved chlorine-isotope fine structure and the

<sup>5</sup> See, for example, H. E. Hallam, 'Vibrational Spectroscopy of Trapped Species,' Wiley, 1973.

<sup>6</sup> C. G. Barraclough and D. Everett, personal communication.

<sup>7</sup> I. R. Beattie and J. R. Horder, *J. Chem. Soc. (A)*, 1969, 2655.

<sup>8</sup> G. O. Jones and J. M. Woodfine, *Proc. Phys. Soc.*, 1965, **86**, 101.

importance of this in connection with the band at  $620\text{ cm}^{-1}$  is discussed below.

Figures 2(c) and 2(d) show the effect of superheating<sup>9</sup> aluminium chloride vapour to a temperature of *ca.* 920 K before deposition with argon. The Raman spectrum, 2(c), shows seven  $\text{Al}_2\text{Cl}_6$  features, and, in addition, two prominent bands at  $392$  and  $150\text{ cm}^{-1}$ . The latter bands were both examined under optimum resolution, and,

position, and the growth of this new feature as a function of superheater temperature is shown in the high-resolution spectra 2(f)—2(h). The spectrum in Figure 2(f) was obtained at a superheater temperature of 400 K and shows the chlorine-isotope fine structure on the  $\text{Al}_2\text{Cl}_6$  band at *ca.*  $620\text{ cm}^{-1}$ , with the four most prominent components at  $621.5$ ,  $620.5$ ,  $618.0$ , and  $616.8\text{ cm}^{-1}$ . Two weak features are also present at  $618.8$  and  $615.2\text{ cm}^{-1}$ .

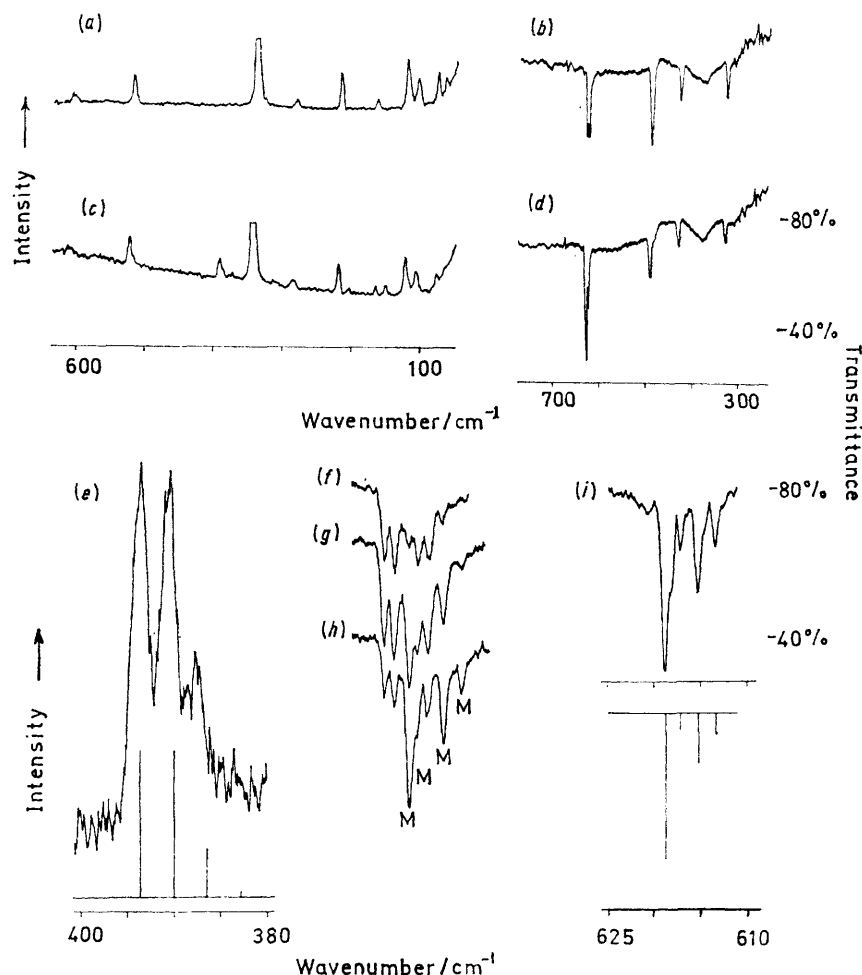


FIGURE 2 Vibrational spectra of aluminium trichloride isolated in argon matrices at 12 K. (a), Raman spectrum without superheating; (b), corresponding i.r. spectrum; (c), Raman spectrum after superheating to 920 K; (d), corresponding i.r. spectrum; (e), high-resolution Raman spectrum; (f)—(i), high-resolution i.r. spectra ( $610$ — $625\text{ cm}^{-1}$ ) at superheater temperatures of 400, 750, 1 000, and 1 000 K (in the presence of metallic gallium) respectively

although it was not possible to detect chlorine-isotope fine structure on the lower band, the  $392\text{ cm}^{-1}$  band could be resolved into three components at  $393.5$ ,  $390.5$ , and  $387.3\text{ cm}^{-1}$  with the approximate intensity ratios 3 : 3 : 1 [Figure 2(e)]. These new bands at *ca.*  $392$  and  $150\text{ cm}^{-1}$  are provisionally assigned to matrix-isolated  $\text{AlCl}_3$  monomer.

The effect of superheating in the i.r. experiments is to produce an apparent enhancement of the band at *ca.*  $620\text{ cm}^{-1}$ , and this is shown in Figure 2(d). This change in the spectrum is due to the appearance of a new band which almost exactly overlaps the  $\text{Al}_2\text{Cl}_6$  band at this

position, and the growth of this new feature as a function of superheater temperature is shown in the high-resolution spectra 2(f)—2(h). The spectrum in Figure 2(f) was obtained at a superheater temperature of 400 K and shows the chlorine-isotope fine structure on the  $\text{Al}_2\text{Cl}_6$  band at *ca.*  $620\text{ cm}^{-1}$ , with the four most prominent components at  $621.5$ ,  $620.5$ ,  $618.0$ , and  $616.8\text{ cm}^{-1}$ . Two weak features are also present at  $618.8$  and  $615.2\text{ cm}^{-1}$ . Figure 2(h) shows the same spectral region under the same slit conditions in an experiment with the superheater at 1 000 K, and it is evident that the peaks at  $618.8$  and  $615.2\text{ cm}^{-1}$  are now the most intense features, and that two further peaks have appeared at  $617.0$  and  $613.3\text{ cm}^{-1}$ . These four bands are assigned to monomeric  $\text{AlCl}_3$  and designated 'M' on this spectrum. The spectrum shown in Figure 2(g) was obtained at the intermediate superheater temperature of *ca.* 750 K.

Figure 2(i) shows the effect of passing aluminium

<sup>9</sup> G. E. Vrieland and D. R. Stull, *J. Chem. and Eng. Data*, 1967, 12, 532.

chloride vapour through the superheater at 1 000 K containing a small amount of metallic gallium. The products were condensed with an excess of argon at 12 K, and the i.r. spectrum in this region showed essentially only the four components assigned to  $\text{AlCl}_3$ . A detailed discussion of this isotope pattern is given below and in the Appendix. When the intensity of the most intense component at  $618.8\text{ cm}^{-1}$  was allowed to build up to full scale, no corresponding absorption was observed in the frequency region at  $360\text{--}400\text{ cm}^{-1}$ , and this suggests that the band found in the Raman at  $392\text{ cm}^{-1}$  is effectively forbidden in the i.r.

In addition to the bands assigned to  $\text{Al}_2\text{Cl}_6$  and  $\text{AlCl}_3$ , several of the i.r. spectra showed traces of matrix-isolated HCl and water, and in some spectra a weak band was occasionally observed at  $598\text{ cm}^{-1}$ . This band was not present in the experiments shown in Figures 2(b) and 2(d), and in the few experiments in which it assumed any prominence (optical density *ca.* 0.05) it was observed to grow only in the initial stages of sample deposition.

**Spectral interpretation:**  $\text{Al}_2\text{Cl}_6$ . The i.r. and Raman fundamentals reported here for matrix-isolated  $\text{Al}_2\text{Cl}_6$  show small frequency shifts from the earlier gas-phase values reported by Klemperer<sup>10</sup> and by Beattie and Horder<sup>7</sup> (Table 1). In addition, there is also qualitative agreement with the argon-matrix i.r. spectrum obtained by Lesiecki and Shirk.<sup>2</sup> However, our interpretation of the matrix-isolation spectrum of  $\text{Al}_2\text{Cl}_6$  differs in two significant respects from that given in Lesiecki and Shirk's paper.

First, although the frequencies reported here are very close to those observed by Lesiecki and Shirk, these authors assign only three of these bands as fundamentals of  $\text{Al}_2\text{Cl}_6$  and dismiss the band at  $320\text{ cm}^{-1}$  as an impurity. In our experiments, this particular band was always present with approximately the same intensity as the band at  $421\text{ cm}^{-1}$  and we have no reason to suppose that it is anything but a genuine  $\text{Al}_2\text{Cl}_6$  fundamental. A possible assignment would be the  $B_{3u}$  stretching mode,  $\nu_{17}$ . This band was not reported by Klemperer (Table 1), but this is presumably because his experiments did not extend below  $325\text{ cm}^{-1}$ . As is seen in Table 1, this assignment is quite consistent with a parallel interpretation of the spectrum of matrix-isolated  $\text{Ga}_2\text{Cl}_6$ .

The second point concerns the intensity of the band at  $620\text{ cm}^{-1}$  compared with the other fundamentals of  $\text{Al}_2\text{Cl}_6$ . As indicated above, Lesiecki and Shirk find this to be the most intense i.r. absorption, whereas we note that it is slightly less intense than the band at  $482\text{ cm}^{-1}$ . This may be simply a feature of different instrumental conditions, but it could be accounted for if a small proportion of monomer were present in Lesiecki and Shirk's  $\text{Al}_2\text{Cl}_6$  spectrum. The proportion of  $\text{AlCl}_3$  present in the vapour phase at temperatures below 500 K is expected<sup>9</sup> to be vanishingly small under normal conditions, but an approximate calculation

using the available thermodynamic data<sup>9</sup> indicates that up to *ca.* 10% monomer might be present in the vapour if the total pressure in the system is very low, *e.g.*  $10^{-7}$  Torr. This pressure could easily be achieved close to the deposition surface. Support for this explanation comes from the observation that our high-resolution spectrum of the dimer band at *ca.*  $620\text{ cm}^{-1}$  shows a weak component at  $618.8\text{ cm}^{-1}$  [Figure 2(f)] which is identified as a monomer absorption on the basis of subsequent superheating experiments.

Table 1 compares the  $\text{Al}_2\text{Cl}_6$  fundamentals observed in this work with earlier studies, and the nomenclature used in the assignment follows that originally suggested by Bell and Longuet-Higgins.<sup>11</sup> Several of the assignments, however, must still be regarded as tentative, as a number of fundamentals of molecular  $\text{Al}_2\text{Cl}_6$  have yet to be located. In particular, there seems to be no satisfactory assignment for the band at  $77\text{ cm}^{-1}$  which is observed both in this work and in the gas phase and has also been reported in the melt.<sup>12</sup> The band at  $283\text{ cm}^{-1}$  has not yet been observed in the gas phase, but it has been located in the Raman spectrum of the melt, and has been assigned by Klemperer<sup>10</sup> as a possible combination band. This assignment would be consistent with its rather low intensity in the matrix.

$\text{AlCl}_3$ . The superheating experiments on  $\text{Al}_2\text{Cl}_6$  produced two additional bands in the Raman spectrum at *ca.*  $392$  and *ca.*  $150\text{ cm}^{-1}$ , and one extra band in the i.r. ( $200\text{--}4\,000\text{ cm}^{-1}$ ) at *ca.*  $618\text{ cm}^{-1}$ . The bands at  $392$  and  $618\text{ cm}^{-1}$  show isotope fine structure, and in an earlier letter<sup>4</sup> we briefly stated why we regard these results as indicating that molecular  $\text{AlCl}_3$  has  $D_{3h}$  symmetry. It now remains to justify this interpretation in detail.

As a prerequisite to any discussion about molecular geometry, it must first be established that these three bands arise from monomeric  $\text{AlCl}_3$ , and a comparison with the previous high-temperature vapour-phase studies on  $\text{AlCl}_3$  is instructive. Beattie and Horder<sup>7</sup> observed two Raman-active bands at *ca.*  $371$  and *ca.*  $146\text{ cm}^{-1}$  which, with the aid of depolarisation measurements, were assigned as the totally symmetric stretching mode ( $A_1'$ ) and the  $E'$  in-plane bending mode of monomeric  $\text{AlCl}_3$ . These bands are quite close to the Raman bands observed here. The high-temperature i.r. study by Klemperer<sup>10</sup> yielded one monomer fundamental at *ca.*  $610\text{ cm}^{-1}$  in the frequency range at  $325\text{--}1\,200\text{ cm}^{-1}$ , and this was assigned as the  $E'$  antisymmetric stretching vibration. This band is also very close to the argon-matrix i.r. band observed in this work. There is therefore substantial agreement between our results and the two previous gas-phase studies on monomeric  $\text{AlCl}_3$ , both of which were consistent with a  $D_{3h}$  geometry.

The most important method of characterisation, however, depends on the interpretation of the isotope fine structure on the bands at  $392$  and  $618\text{ cm}^{-1}$ . Aluminium has only one naturally occurring isotope and the natural abundance ratio of the two chlorine isotopes  $^{35}\text{Cl}$  and

<sup>10</sup> W. Klemperer, *J. Chem. Phys.*, 1956, **24**, 353.

<sup>11</sup> R. P. Bell and H. C. Longuet-Higgins, *Proc. Roy. Soc.*, 1945, **A183**, 357.

<sup>12</sup> E. V. Pershina and Sh. Sh. Raskin, *Optics and Spectroscopy*, 1962, **13**, 272.



$^{37}\text{Cl}$  is *ca.* 3:1. For  $D_{3h}$  or  $C_{3v}$  symmetry, the four molecular species  $\text{Al}^{35}\text{Cl}_3$ ,  $\text{Al}^{35}\text{Cl}_2^{37}\text{Cl}$ ,  $\text{Al}^{35}\text{Cl}^{37}\text{Cl}_2$ , and  $\text{Al}^{37}\text{Cl}_3$  will therefore have relative abundances of *ca.* 27:27:9:1, *i.e.* *ca.* 3:3:1:0.1. Under high resolution, a non-degenerate vibration of  $\text{AlCl}_3$ , such as the symmetric stretching mode, would therefore be expected to show four closely spaced components with these approximate intensity ratios, and we assign the triplet pattern in Figure 2(e) to the three most intense components of this expected quartet. This assignment is strongly supported by the isotope-frequency calculations, and the line diagram accompanying this spectrum is a very satisfactory fit. A degenerate vibration such as the antisymmetric stretching mode would show a more complicated pattern due to the removal of this degeneracy in the partially substituted molecules. This pattern can, however, be calculated as shown in the Appendix, and it turns out that the calculated isotope pattern for this mode is very close indeed to that observed experimentally [Figure 2(i)]. The ultimate decision as to whether  $\text{AlCl}_3$  has  $D_{3h}$  or  $C_{3v}$  symmetry then rests partly on vibrational selection rules and partly on the results of the force-constant analyses, and two experimental observations are relevant here.

In the first place it must be noted that the band at 392  $\text{cm}^{-1}$ , which is prominent in the Raman, was not observed at all in our i.r. studies even though the component at 618.8  $\text{cm}^{-1}$  was allowed to build up to full-scale absorbance (0% transmittance). It is impossible to place an accurate estimate on the intensity factor involved here, but simple optical-density considerations suggest that if the band at 392  $\text{cm}^{-1}$  were active in the i.r. the absorption coefficient cannot be greater than *ca.* 0.5% of that for the component at 618.8  $\text{cm}^{-1}$ . The second experimental observation concerns the bending mode,  $\nu_2$ . This band was not observed in our i.r. studies, but it may be expected to lie in the range 100–200  $\text{cm}^{-1}$ , and has in fact been reported to lie at *ca.* 183  $\text{cm}^{-1}$  by Lesiecki and Shirk.<sup>2</sup> We are unable to confirm this assignment, but if  $\text{AlCl}_3$  were in fact pyramidal, this 'out of plane vibration' would become the totally symmetric bending mode, and might therefore be expected to be observed in the Raman studies. It has not so far been reported.

Finally, we have the quantitative results of the force-constant calculations. These are described in the Appendix, and were made first to reproduce the frequencies of all the in-plane fundamentals of the  $\text{AlCl}_3$  isotope species, and secondly to reproduce the frequencies and relative i.r. band intensities of the stretching modes. A planar  $D_{3h}$  structure was assumed for both sets of calculations. As indicated above, the line diagrams accompanying the high-resolution spectra, and the actual wavenumber agreement (Table 2), are both very satisfactory, and, although one should not place too much reliance on the significance of the numerical values of potential constants derived from approximate force fields, it is interesting to note what effects are produced if one arbitrarily fixes the

\* This estimate of the  $A_1$  intensity was made using the bond-dipole approach outlined in the Appendix.

$\text{Cl-Al-Cl}$  bond angle at an equilibrium value of less than *ca.* 115°. Not only must the interaction constant  $F_{RR}$  be given a negative value, but also the totally symmetric stretching mode (now active in the i.r.) would be expected\* to have an absorption coefficient >3% of that of the component at 618.8  $\text{cm}^{-1}$ .

TABLE 2

Observed and calculated wavenumbers ( $\text{cm}^{-1}$ ) for monomeric  $\text{AlCl}_3$

	Observed		Calculated		Assignment
	Vapour <sup>7</sup>	Ar matrix <sup>a</sup>	(I) <sup>b</sup>	(II) <sup>c</sup>	
(610) <sup>10</sup>		618.8	618.80	618.80	$E' \text{ Al}^{35}\text{Cl}_3$
			618.78	618.80	$B_2 \text{ Al}^{35}\text{Cl}_2^{37}\text{Cl}$
		617.0	617.11	616.95	$A_1 \text{ Al}^{35}\text{Cl}^{37}\text{Cl}_2$
		615.2	615.45	615.05	$A_1 \text{ Al}^{35}\text{Cl}_2^{37}\text{Cl}$
371		613.3	613.69	613.09	$B_2 \text{ Al}^{35}\text{Cl}^{37}\text{Cl}_2$
			613.67	613.09	$E' \text{ Al}^{37}\text{Cl}_3$
		393.5	393.50	393.50	$A_1' \text{ Al}^{35}\text{Cl}_3$
		390.5	389.88	389.85	$A_1 \text{ Al}^{35}\text{Cl}_2^{37}\text{Cl}$
146		387.3	386.29	386.27	$A_1 \text{ Al}^{35}\text{Cl}^{37}\text{Cl}_2$
			382.72	382.72	$A_1' \text{ Al}^{37}\text{Cl}_3$
	150		152.00		$E' \text{ Al}^{35}\text{Cl}_3$
	(broad)		148.24		$E' \text{ Al}^{37}\text{Cl}_3$

<sup>a</sup> Accuracy,  $\pm 0.5 \text{ cm}^{-1}$ . <sup>b</sup> Using the parameters  $F_R = 2.7572$ ,  $F_{RR} = 0.2174$ , and  $F_{\theta/R^2} = 0.1009 \text{ mdyn } \text{\AA}^{-1}$ . <sup>c</sup> Using the parameters  $F_R = 2.8513$ ,  $F_{RR} = 0.1704$ , and  $F_{\theta/R^2} = 0 \text{ mdyn } \text{\AA}^{-1}$ .

On the basis of these results, we therefore believe that  $\text{AlCl}_3$  has a planar  $D_{3h}$  structure. Lesiecki and Shirk's conclusions that  $\text{AlCl}_3$  has  $C_{3v}$  symmetry are based on frequencies which we are unable to reproduce and which we believe are not fundamentals of  $\text{AlCl}_3$ . Lesiecki and Shirk's spectrum can be understood if they have in fact observed the fundamentals of an adduct such as  $\text{AlCl}_3 \cdot \text{M}$ . Here one might expect to have a pyramidal  $\text{AlCl}_3$  unit (*cf.*  $\text{AlCl}_3 \cdot \text{NH}_3$ <sup>13</sup>) and the symmetric Al-Cl stretching mode would be active in the i.r. In putting forward this interpretation we note that the deposition times of *ca.* 30 h used in Lesiecki and Shirk's experiments are greater by over an order of magnitude than those used in this work, and with such extended depositions one might anticipate problems arising from the natural degassing rate of adsorbed species from the room-temperature walls of the apparatus. The  $D_{3h}$  structure derived here for  $\text{AlCl}_3$  supports the original electron-diffraction studies of Zasorin and Rambidi,<sup>8</sup> and is also consistent with the recent *ab initio* calculations of So and Richards.<sup>14</sup>

**Gallium Trichloride.**—Gallium trichloride is slightly volatile at ambient temperatures, and the matrix-isolation Raman spectrum shown in Figure 3(a) was obtained by co-condensing gallium trichloride vapour warmed to 300 K with a large excess of argon. The argon lattice mode<sup>8</sup> was again visible at 65  $\text{cm}^{-1}$  and bands were also observed at 467, 416, 345, 322, 239, 167, 115, 100, and 77  $\text{cm}^{-1}$  which are attributed to the dimer

<sup>13</sup> M. Hargittai, I. Hargittai, V. P. Spiridonov, M. Pelissier, and J.-F. Laharre, *J. Mol. Struct.*, 1975, **24**, 27.

<sup>14</sup> S. P. So and W. G. Richards, *Chem. Phys. Letters*, 1975, **32**, 231.

$\text{Ga}_2\text{Cl}_6$ . The corresponding i.r. spectrum [Figure 3(b)] showed four bands at 468, 399, 311, and 281  $\text{cm}^{-1}$ . Our identification of these bands as fundamentals of  $\text{Ga}_2\text{Cl}_6$  is based on a comparison of these spectra with the earlier work of Beattie *et al.*,<sup>15</sup> and Table 1 shows the extent of this agreement together with tentative assignments.

Figures 3(c) and 3(d) show the effect of superheating in this system. In the Raman experiments, the vapour was

sensitivity [*e.g.* Figure 2(d)] but no band was ever observed in the region of the Raman feature at 384  $\text{cm}^{-1}$ . By comparison with the previous results on  $\text{AlCl}_3$ , these new bands are provisionally assigned to monomeric  $\text{GaCl}_3$  with  $D_{3h}$  symmetry.

Prior to these experiments, the only vibrational data on molecular  $\text{GaCl}_3$  was the high-temperature vapour-phase Raman study by Beattie and Horder.<sup>7</sup> This work established that the totally symmetric ( $A_1'$ ) stretching

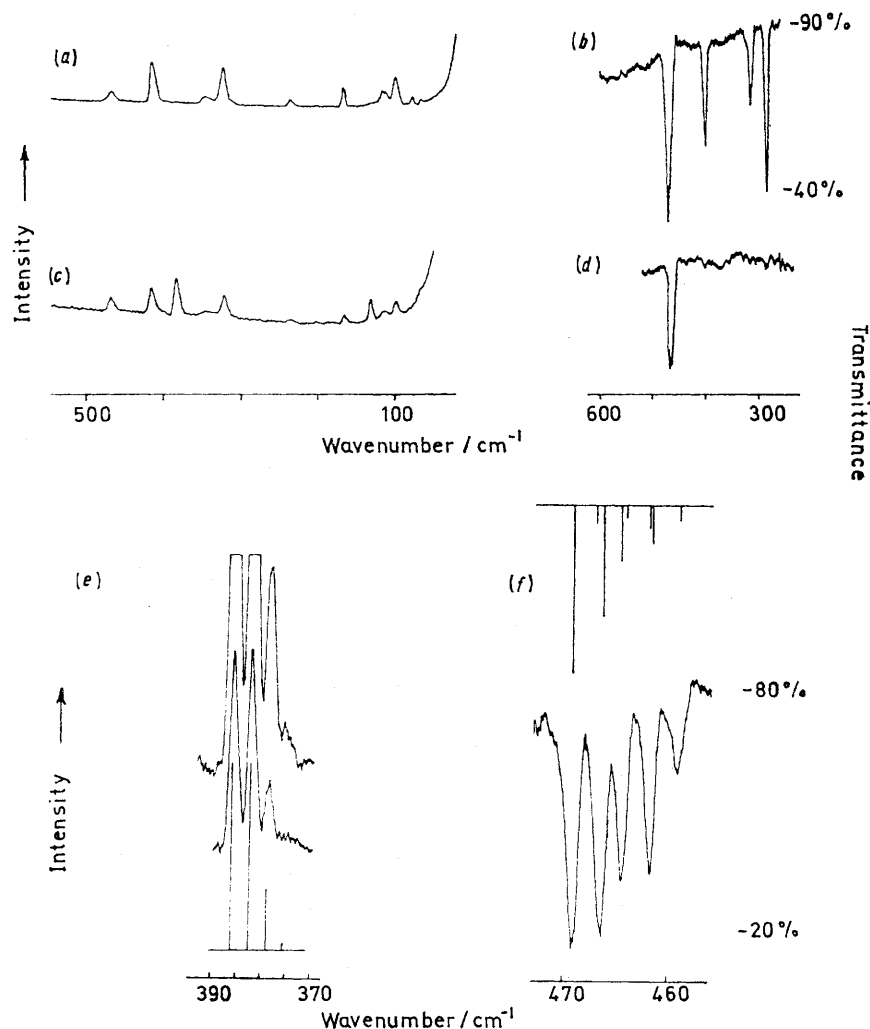


FIGURE 3 Vibrational spectra of gallium trichloride isolated in argon matrices at 12 K. (a), Raman spectrum without superheating; (b), corresponding i.r. spectrum; (c), Raman spectrum after superheating to 900 K; (d), corresponding i.r. spectrum; (e), high-resolution Raman spectrum; (f), high-resolution i.r. spectrum

heated to *ca.* 900 K and, although bands due to  $\text{Ga}_2\text{Cl}_6$  are still present, it is evident that there are two new features at *ca.* 384 and *ca.* 132  $\text{cm}^{-1}$ , and that the band at 467  $\text{cm}^{-1}$  is enhanced in intensity. The corresponding superheating experiments in the i.r. produced essentially only one band in the frequency range at 200–4 000  $\text{cm}^{-1}$ , and this was centred at *ca.* 468  $\text{cm}^{-1}$ . Weak residual dimer features were sometimes detected under increased

mode lies at 382  $\text{cm}^{-1}$  and the  $E'$  in-plane bending mode at 128  $\text{cm}^{-1}$ . The antisymmetric stretching mode, although active in the Raman, was expected to be weak and was not observed. In the matrix-Raman experiments described here two new features were clearly observed after superheating at 384 and 132  $\text{cm}^{-1}$ , and these appear to be associated with a third, weaker, feature at *ca.* 467  $\text{cm}^{-1}$  overlapping the  $\text{Ga}_2\text{Cl}_6$  fundamental. These results are therefore in agreement with the vapour-phase Raman data if one assigns this third

<sup>15</sup> I. R. Beattie, T. R. Gilson, and P. Cocking, *J. Chem. Soc. (A)*, 1967, 702.

band as the  $E'$  antisymmetric stretching mode. This assignment is supported by the observation of an intense band centred at  $467\text{ cm}^{-1}$  in the i.r. spectrum [Figure 3(d)], and the identification of these bands as fundamentals of  $D_{3h}$   $\text{GaCl}_3$  is further strengthened by the isotope patterns observed under high resolution.

Figures 3(e) and 3(f) show the bands at  $384\text{ cm}^{-1}$  (Raman) and at  $467\text{ cm}^{-1}$  (i.r.) under optimum resolution, and it is clear that whereas the Raman spectrum shows the expected intensity variation for a  $D_{3h}$  trichloride, the i.r. spectrum shows an unusual five-line pattern which cannot immediately be assigned and requires further discussion. Under high resolution the fundamental vibrations of  $\text{GaCl}_3$  will, in principle, show fine structure arising not only from the two chlorine isotopes but also from the two isotopes of gallium,  $^{69}\text{Ga}$  and  $^{71}\text{Ga}$ , which are present in natural abundance in the ratio *ca.* 3 : 2. In practice, the effect on the observed spectra will depend basically on the extent to which the gallium atom is involved in the two modes under investigation and a comparison with  $\text{BCl}_3$  is relevant here.

It is well known that the totally symmetric stretching mode in  $\text{BCl}_3$  shows characteristic chlorine isotope structure,<sup>16</sup> but a boron isotope effect has never been detected for this vibration. This is because<sup>16</sup> the central atom does not move at all in a truly  $D_{3h}$  species such as  $\text{B}^{35}\text{Cl}_3$ , and in the partially substituted  $C_{2v}$  species it may be shown that the movement is very small in the related symmetric stretch. The net effect is thus a superposition of the chlorine-isotope quartets for  $^{10}\text{BCl}_3$  and  $^{11}\text{BCl}_3$  and one would expect an analogous situation to exist here in the high-resolution Raman spectrum of the  $A_1$  mode in  $\text{GaCl}_3$ . The intensity pattern in Figure 3(e) clearly confirms this. In contrast, the antisymmetric stretching mode involves appreciable central-atom movement, and for  $\text{BCl}_3$  the quartet patterns characteristic of this mode are well resolved for both  $^{10}\text{BCl}_3$  and  $^{11}\text{BCl}_3$  [Figure 5(a)] and are separated by *ca.*  $40\text{ cm}^{-1}$ . The corresponding antisymmetric mode in  $\text{GaCl}_3$  should therefore also appear as two quartets. Simple product-rule calculations show, however, that the gallium isotope effect is the same order of magnitude as the chlorine-isotope splitting and the two quartets are therefore expected to overlap. More extensive calculations (see Appendix) allow one to predict the frequencies and relative intensities of each isotope component and the results of these calculations for  $^{69}\text{GaCl}_3$  and  $^{71}\text{GaCl}_3$  are shown in the line diagram accompanying Figure 3(f). The unusual five-line spectrum is thus seen to arise as a result of overlap between three of the components of the  $^{69}\text{Ga}$  quartet and three of the components of the  $^{71}\text{Ga}$  quartet. The wavenumber agreement shown in Table 3 is again very satisfactory.

**Indium Trichloride.**—The matrix isolation of indium trichloride vapour sublimed at *ca.*  $650\text{ K}$  gives relatively simple Raman and i.r. spectra, and these are shown in Figures 4(a) and 4(b). Only three bands were observed in the Raman spectrum, at  $400$ , *ca.*  $357$ , and *ca.*  $119\text{ cm}^{-1}$

[Figure 4(a)], and only one band was observed in the corresponding i.r. studies [Figure 4(b)] at *ca.*  $400\text{ cm}^{-1}$ . Under high resolution, the Raman band at  $357\text{ cm}^{-1}$  and the i.r. band at  $400\text{ cm}^{-1}$  showed isotope patterns characteristic of a monomeric trichloride. No fine structure was detected which could be assigned to different indium isotopes. On the evidence of these spectra, there seems little doubt that the only species present in the matrix

TABLE 3  
Observed and calculated wavenumbers ( $\text{cm}^{-1}$ ) for monomeric  $\text{GaCl}_3$

Observed	Calculated		Assignment
	(I) <sup>b</sup>	(II) <sup>c</sup>	
Vapour <sup>a</sup>			
Ar matrix <sup>a</sup>			
469.3	469.30	469.30	$E'$ $^{69}\text{Ga}^{35}\text{Cl}_3$
	469.29	469.30	$B_2$ $^{69}\text{Ga}^{35}\text{Cl}_3^{37}\text{Cl}$
	467.15	467.07	$A_1$ $^{69}\text{Ga}^{35}\text{Cl}_3^{37}\text{Cl}_2$
466.5	466.28	466.44	$E'$ $^{71}\text{Ga}^{35}\text{Cl}_3$
	466.27	466.44	$B_2$ $^{71}\text{Ga}^{35}\text{Cl}_3^{37}\text{Cl}$
	464.86	464.66	$A_1$ $^{69}\text{Ga}^{35}\text{Cl}_3^{37}\text{Cl}$
464.5	464.12	464.20	$A_1$ $^{71}\text{Ga}^{35}\text{Cl}_3^{37}\text{Cl}_2$
	462.35	462.04	$B_2$ $^{69}\text{Ga}^{35}\text{Cl}_3^{37}\text{Cl}_2$
461.8	462.34	462.04	$E'$ $^{69}\text{Ga}^{37}\text{Cl}_3$
	461.82	461.77	$A_1$ $^{71}\text{Ga}^{35}\text{Cl}_3^{37}\text{Cl}$
	459.28	459.13	$B_2$ $^{71}\text{Ga}^{35}\text{Cl}_3^{37}\text{Cl}_2$
459.0	459.27	459.13	$E'$ $^{71}\text{Ga}^{37}\text{Cl}_3$
	386.20	386.20	$A_1'$ $\text{Ga}^{35}\text{Cl}_3$
382	382.49	382.48	$A_1$ $\text{Ga}^{35}\text{Cl}_3^{37}\text{Cl}$
	379.2	378.96	$A_1$ $\text{Ga}^{35}\text{Cl}_3^{37}\text{Cl}_2$
	375.7	375.62	$A_1'$ $\text{Ga}^{37}\text{Cl}_3$
128	132	133.00	$E'$ $^{69}\text{Ga}^{35}\text{Cl}_3$
	(broad)	129.61	$E'$ $^{71}\text{Ga}^{37}\text{Cl}_3$

<sup>a</sup> Accuracy,  $\pm 0.5\text{ cm}^{-1}$ . <sup>b</sup> Using the parameters  $F_R = 2.7086$ ,  $F_{RR} = 0.1831$ , and  $F_{\theta/R^2} = 0.0867\text{ mdyn Å}^{-1}$ . <sup>c</sup> Using the parameters  $F_R = 2.7438$ ,  $F_{RR} = 0.1654$ , and  $F_{\theta/R^2} = 0\text{ mdyn Å}^{-1}$ .

under these conditions is monomeric  $\text{InCl}_3$ , and this observation may be contrasted with previous vapour-phase studies on this system.<sup>7</sup>

The high-temperature Raman work by Beattie and Horder<sup>7</sup> was carried out at a sample pressure of *ca.*  $760\text{ Torr}$ , and at  $570^\circ\text{C}$  prominent bands were observed at  $368$ ,  $298$ , and *ca.*  $70\text{ cm}^{-1}$  which were assigned to  $\text{In}_2\text{Cl}_6$ . On further heating these bands decreased in intensity, and prominent features assigned to monomeric  $\text{InCl}_3$  were  $350$  and  $94\text{ cm}^{-1}$ . The band at  $94\text{ cm}^{-1}$  was very broad, and partially overlapped by residual dimer. Our matrix-Raman spectra show no trace of  $\text{In}_2\text{Cl}_6$ , and the corresponding simplicity of the i.r. spectrum suggests that in both types of experiment the pressure during deposition (*ca.*  $10^{-3}\text{ Torr}$ ) is sufficiently low to cause complete dissociation,  $\text{In}_2\text{Cl}_6 \rightarrow 2\text{InCl}_3$ . It is perhaps relevant that solid anhydrous  $\text{InCl}_3$  does not contain molecular  $\text{In}_2\text{Cl}_6$  units.<sup>17</sup> The observation of only one absorption in the i.r. spectrum ( $200\text{--}4000\text{ cm}^{-1}$ ) strongly suggests that  $\text{InCl}_3$  is a planar  $D_{3h}$  molecule, and it is evident from Figure 4(a) that this  $E'$  stretching mode is also present in the Raman spectrum. This coincidence of fundamentals is expected according to  $D_{3h}$  selection rules, but it is only for  $\text{InCl}_3$  that it may be unambiguously observed,

<sup>16</sup> R. J. H. Clark and P. D. Mitchell, *J. Chem. Phys.*, 1972, **56**, 2225.

<sup>17</sup> D. H. Templeton and G. F. Carter, *J. Phys. Chem.*, 1954, **58**, 940.

since our Raman spectra of the aluminium and gallium chloride systems both show dimer bands in the region of this  $E'$  monomer fundamental.

Table 4 compares the wavenumbers observed in this

the usefulness of the two-parameter potential function in the calculation of i.r. isotope frequencies and relative band intensities.

**Conclusions.**—There is no evidence from the results

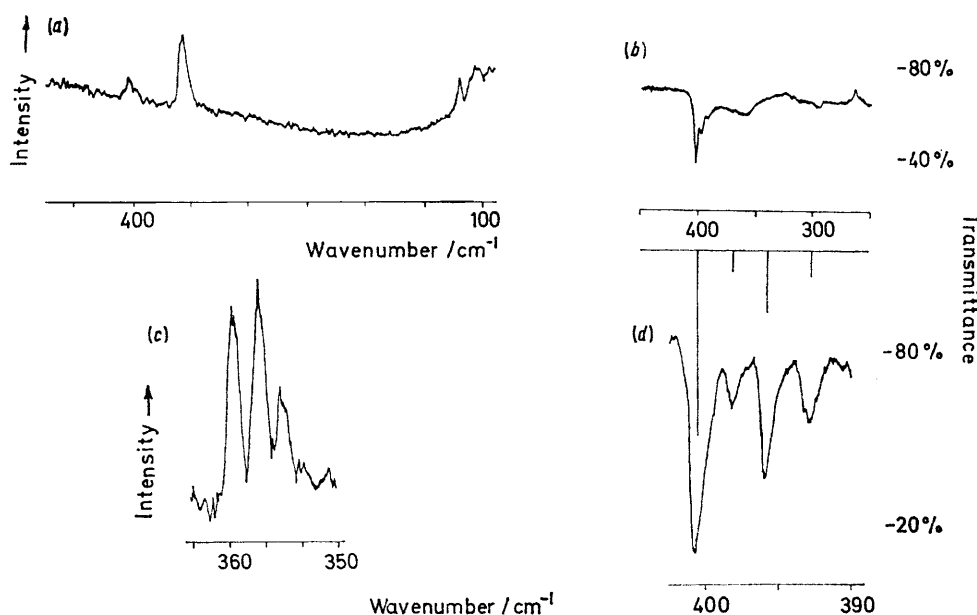


FIGURE 4 Vibrational spectra of indium trichloride isolated in argon matrices at 12 K. (a), Raman spectrum; (b), corresponding i.r. spectrum; (c), high-resolution Raman spectrum; (d), high-resolution i.r. spectrum

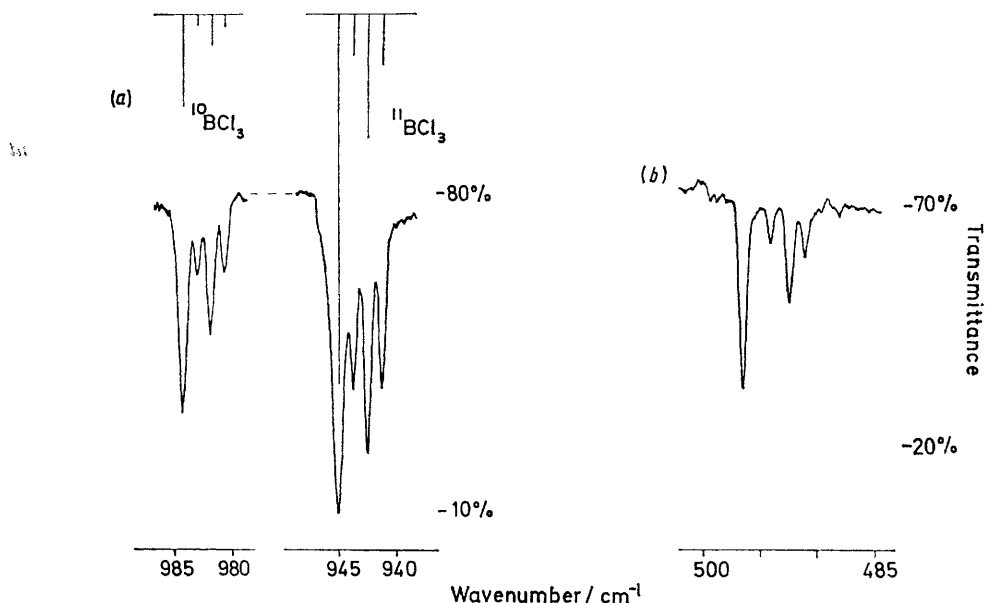


FIGURE 5 (a), High-resolution i.r. spectrum of the antisymmetric stretching mode of  $\text{BCl}_3$  isolated in an argon matrix at 12 K; (b), high-resolution i.r. spectrum of the antisymmetric stretching mode of  $\text{PCl}_3$  isolated in a nitrogen matrix at 12 K

work with the previous gas-phase data on monomeric  $\text{InCl}_3$  and with the isotope wavenumbers calculated assuming a  $D_{3h}$  model. The agreement is very satisfactory, and the line diagram accompanying the high-resolution spectrum of  $\text{InCl}_3$  in Figure 4(d) again shows

described in this paper that the three species  $\text{AlCl}_3$ ,  $\text{GaCl}_3$ , and  $\text{InCl}_3$  show any significant departure from  $D_{3h}$  symmetry, and it is therefore interesting to compare these conclusions first with related studies on other Group 3 trihalides and secondly with the corresponding



Group 2 dihalides. All the boron halides are planar, and  $\text{AlF}_3$ <sup>18</sup> and  $\text{GaF}_3$ <sup>19</sup> are also believed to be planar. In contrast, there is evidence that  $\text{YF}_3$  and  $\text{LaF}_3$  are pyramidal,<sup>20</sup> and if this is so one might anticipate structural differences analogous to those found in the Group 2 halides. As indicated earlier,<sup>1</sup> all the dihalides of beryllium (and magnesium<sup>21</sup>) appear to be linear, but

TABLE 4  
Observed and calculated wavenumbers ( $\text{cm}^{-1}$ ) for monomeric  $\text{InCl}_3$

Vapour <sup>7</sup>	Observed	Calculated		Assignment
	Ar matrix <sup>a</sup>	(I) <sup>b</sup>	(II) <sup>c</sup>	
	400.5	400.50	400.50	$E'$ $\text{In}^{35}\text{Cl}_3$
	398.5	400.49	400.50	$B_2$ $\text{In}^{35}\text{Cl}_2^{37}\text{Cl}$
	396.0	398.39	398.35	$A_1$ $\text{In}^{35}\text{Cl}^{37}\text{Cl}_2$
		396.01	395.90	$A_1$ $\text{In}^{35}\text{Cl}_2^{37}\text{Cl}$
	393.0	393.17	393.00	$B_2$ $\text{In}^{35}\text{Cl}^{37}\text{Cl}_2$
		393.17	393.00	$E'$ $\text{In}^{37}\text{Cl}_3$
	359.0	359.00	359.00	$A_1'$ $\text{In}^{35}\text{Cl}_3$
350	355.5	355.33	355.32	$A_1$ $\text{In}^{35}\text{Cl}_2^{37}\text{Cl}$
	352.5	352.10	352.09	$A_1$ $\text{In}^{35}\text{Cl}^{37}\text{Cl}_2$
	349.5	349.16	349.16	$A_1'$ $\text{In}^{37}\text{Cl}_3$
ca. 94	119 (broad)	120.00		$E'$ $\text{In}^{35}\text{Cl}_3$
		117.2		$E'$ $\text{In}^{37}\text{Cl}_3$

<sup>a</sup> Accuracy,  $\pm 0.5 \text{ cm}^{-1}$ . <sup>b</sup> Using the parameters  $F_R = 2.3818$ ,  $F_{RR} = 0.1375$ , and  $F_{\theta/R^2} = 0.0761 \text{ m dyn } \text{\AA}^{-1}$ . <sup>c</sup> Using the parameters  $F_R = 2.3983$ ,  $F_{RR} = 0.1293$ , and  $F_{\theta/R^2} = 0 \text{ m dyn } \text{\AA}^{-1}$ .

$C_{2v}$  geometries become increasingly important for the heavier metal halides in the pre-transition Group 2A. In contrast, all the dihalides in Group 2B (Zn to Hg) are linear. If this A-B structural divergence is the result of appreciable metal  $d$ -orbital participation<sup>22</sup> in the heavier Group 2A halide, one might predict that all the halides of Group 3B will be planar, but that similar  $d$ -orbital participation in the heavier Group 3A metals will result in pyramidal structures for the 'more ionic' trihalides.

Finally, the conclusions in this paper concerning the shapes of  $\text{MCl}_3$  species have been made primarily on the basis of symmetry selection rules applied to vibrations which can be positively identified as monomer fundamentals, and it is important to examine the extent to which this strategy may be used for the remaining Group 3 trihalides. It will be evident that only for the chlorides will one be able to use halogen-isotope patterns to identify monomer bands, since fluorine and iodine have only one naturally occurring isotope, and only in the most fortunate circumstances<sup>16</sup> would one resolve structure due to  $^{79}\text{Br}$ – $^{81}\text{Br}$ . In the absence of this type of identification, one can anticipate difficulties arising not only from the formation of polymers but also from simple adducts between the highly reactive monomers and trace amounts

of impurity such as water or  $\text{N}_2$ . It will therefore become increasingly important to exploit two additional techniques which are suitable for determining the shapes of molecules at high temperatures, namely electron diffraction and electric deflection. These techniques by themselves have their own difficulties of interpretation, but they are to some extent complementary. In high-temperature electron diffraction<sup>23</sup> the phenomenon of 'shrinkage' will result in all these  $\text{MX}_3$  species appearing pyramidal, and even though one may be able to correct for this the basic parameters obtainable from the scattering curve are not particularly sensitive indications of planarity. This is because small errors in the non-bonded distances  $\text{X} \cdots \text{X}$  produce relatively large deviations from planarity as defined by  $\beta$ , the angle between an M-X bond and the  $C_3$  axis. In their electron-diffraction study on  $\text{AlCl}_3$ , Zasorin and Rambidi calculated the Cl-Al-Cl angle to be  $118 \pm 1.5^\circ$ , but, after taking the estimated shrinkage into effect, concluded that the equilibrium geometry would be planar with  $1^\circ$  of uncertainty. If electron diffraction errs in favour of pyramidal structures, the reverse could be said to hold for electric deflection,<sup>24</sup> since a null result here could be taken as evidence of either a planar molecule or a pyramidal molecule with only a small permanent dipole.

It is therefore apparent that no single technique is free from ambiguities in interpretation, and that a combination of matrix-isolation studies with vapour-phase diffraction and deflection experiments will become increasingly necessary before one can be confident in proposing a particular molecular geometry for many of the remaining trihalides in this Group.

#### APPENDIX

*Isotope Frequencies and Relative I.R. Band Intensities.*—The fundamental vibrations<sup>16</sup> of a  $D_{3h}$   $\text{MX}_3$  are  $A_1' + A_2'' + 2E'$ . The  $A_2''$  vibration is the out-of-plane mode and is active only in the i.r., whilst the  $A_1'$  vibration is the totally symmetric stretching mode and is active only in the Raman. The  $E'$  modes are both i.r. and Raman active, and may be described as the antisymmetric stretching mode and the in-plane bending mode. The most general quadratic force field for this structure requires five independent potential constants, and these may be identified as the principal force constants  $F_R$ ,  $F_\theta$ , and  $F_\Delta$ , and the interaction constants  $F_{RR}$  and  $F_{R\theta}$ , where  $R$  is the M-X bond length,  $\theta$  is the in-plane angle  $\text{XMX}$ , and  $\Delta$  is the angle between an M-X bond and the  $C_3$  axis.

In this paper, we are concerned with the in-plane vibrations of  $\text{MCl}_3$  molecules, and it is clear that four parameters,  $F_R$ ,  $F_{RR}$ ,  $F_\theta$ , and  $F_{R\theta}$ , are required to describe the stretching and bending modes. These parameters may in principle be determined from the observed frequencies of the isotopically pure species  $\text{M}^{35}\text{Cl}_3$  and  $\text{M}^{37}\text{Cl}_3$ , but as we were unable to resolve the chlorine-isotope structure on the  $E'$  bending mode we chose instead to set the interaction constant  $F_{R\theta}$

<sup>18</sup> A. Snelson, *J. Phys. Chem.*, 1967, **71**, 3202.

<sup>19</sup> J. W. Hastie, R. H. Hauge, and J. L. Margrave, *J. Fluorine Chem.*, 1974, **3**, 285.

<sup>20</sup> J. W. Hastie, R. H. Hauge, and J. L. Margrave, personal communication.

<sup>21</sup> R. H. Hauge, J. L. Margrave, and A. S. Kanaan, *J.C.S. Faraday II*, 1975, 1082.

<sup>22</sup> E. F. Hayes, *J. Phys. Chem.*, 1966, **70**, 3740.

<sup>23</sup> See, for example, L. V. Vilkov, N. G. Rambidi, and V. P. Spiridonov, *Zhur. strukt. Khim.*, 1967, **8**, 786.

<sup>24</sup> See, for example, E. W. Kaiser, W. E. Falconer, and W. Klemperer, *J. Chem. Phys.*, 1972, **56**, 5392.

equal to zero and to determine  $F_R$ ,  $F_{RR}$ , and  $F_{\theta/R}$  from the  $M^{35}\text{Cl}_3$  data alone, using the general expressions (A.1)–(A.3)

$$A_1' \quad \lambda_1 = (F_R + 2F_{RR})/X \quad (\text{A.1})$$

$$\lambda_3 + \lambda_4 = (F_R - F_{RR})\left(\frac{1}{X} + \frac{3}{2M}\right) + E' \quad 3F_{\theta/R}\left(\frac{1}{X} + \frac{3}{2M}\right) \quad (\text{A.2})$$

$$\lambda_3\lambda_4 = 3F_{\theta/R}(F_R - F_{RR})\left(\frac{1}{X^2} + \frac{3}{MX}\right) \quad (\text{A.3})$$

in which  $M$  and  $X$  are atomic masses and  $\lambda = 4\pi^2\nu^2$ . These calculated parameters were then used to generate the in-plane vibration frequencies of all the isotopically substituted species  $M^{35}\text{Cl}_n^{37}\text{Cl}_{3-n}$ . These molecules have at least  $C_{2v}$  symmetry, with in-plane stretching modes  $2A_1 + B_2$  and in-plane bending modes  $A_1 + B_2$ , and calculations were therefore made using the standard Wilson  $GF$  method<sup>25</sup> with  $G$  and  $F$  matrices appropriate to these  $\text{MX}_2\text{X}'$  species. Tables 2–4 compare all the wavenumbers observed for  $\text{AlCl}_3$ ,  $\text{GaCl}_3$ , and  $\text{InCl}_3$  with those calculated using this force field [series (I)].

If one further assumes that the antisymmetric stretching modes in these molecules are effectively uncoupled from the in-plane bending modes, it then becomes possible to estimate quantitatively the relative i.r. intensities of the stretching modes in the various isotopically substituted species and so to understand the isotope-intensity patterns observed under high resolution. The general strategy has been described elsewhere,<sup>25</sup> and the procedure adopted here is similar to that described by Darling and Ogden<sup>26</sup> in their analysis of the carbonyl-stretching vibrations of  $D_{3h}$  tricarbonyles. The factoring out of the stretching modes may be achieved by setting  $F_\theta$  equal to zero, and computing new values of  $F_R$  and  $F_{RR}$  from the  $A_1'$  and  $E'$  stretching modes of  $M^{35}\text{Cl}_3$ . These new values are very similar in each case to those obtained for the more general force field above, and this indicates that this separation of the stretching and bending modes is not too gross a simplification. These parameters are then used first to recalculate the frequencies of the stretching modes of isotopically substituted  $M^{35}\text{Cl}_n^{37}\text{Cl}_{3-n}$ , and then to determine relative i.r. band intensities  $I_k$  using the expressions (A.4) and (A.5)<sup>25</sup> in which it is assumed that

$$\sum_k I_k = \sum_{k'k''} \frac{\partial \mu}{\partial S_{k'}} \cdot \frac{\partial \mu}{\partial S_{k''}} \sum_k L_{k'k} L_{k''k} = \sum_{k'k''} \frac{\partial \mu}{\partial S_{k'}} \cdot \frac{\partial \mu}{\partial S_{k''}} G_{k'k''} \quad (\text{A.4})$$

$$\sum_k \frac{I_k}{\lambda_k} = \sum_{k'k''} \frac{\partial \mu}{\partial S_{k'}} \cdot \frac{\partial \mu}{\partial S_{k''}} \sum_k L_{k'k} \lambda_k^{-1} L_{k''k} = \sum_{k'k''} \frac{\partial \mu}{\partial S_{k'}} \cdot \frac{\partial \mu}{\partial S_{k''}} F_{k'k''}^{-1} \quad (\text{A.5})$$

the dipole derivatives,  $\partial \mu / \partial S$ , may be obtained as vector sums of individual bond-dipole derivatives,  $\partial \mu / \partial r$ . Tables 2–4 compare the wavenumbers calculated using this simple

two-parameter force field [series (II)] with those obtained from the more general force field and with the experimental wavenumbers for  $M^{35}\text{Cl}_n^{37}\text{Cl}_{3-n}$ . The relative intensities calculated from the above equations are shown as line spectra in Figures 2–4 after appropriate statistical weighting for the chlorine (and gallium) isotopes.

Some indication of the validity of this approach may be obtained from the agreement which results when this two-parameter force field is used to compute the frequencies and relative intensities of the antisymmetric stretch multiplets in  $\text{BCl}_3$ . Here, we have two boron isotopes in addition to the two isotopes of chlorine, and the experimentally observed eight-line pattern shown in Figure 5 is very closely reproduced by the calculated line spectrum.

Two additional points remain concerning the general application of this kind of analysis. In the first place it is evident that the chlorine isotope patterns observed in this work are all very similar. This similarity does not arise by chance, but is a direct consequence of the in-plane bending mode and the symmetric stretching mode in the parent  $D_{3h}$  molecule being well removed in frequency from the  $E'$  antisymmetric stretching mode. Under these conditions, the intensity of this degenerate mode is shared almost equally between the corresponding  $A_1$  and  $B_2$  components in the partially substituted  $\text{MX}_2\text{X}'$  molecules, and there is negligible intensity borrowing by the other  $A_1$  stretching mode arising from the totally symmetric stretch. The observation of only four lines in this part of the spectrum rather than the expected six arises primarily because of the very weak coupling with the bending modes, which results in a virtual coincidence of the  $B_2$  component with the parent  $E'$  stretching mode. It follows from this that the intensities of the four bands are expected to be in the ratios 81 : 9 : 27 : 11 on the basis of molecular abundances, and these ratios are modified only very slightly<sup>25</sup> if one takes into account the changing isotope mass of chlorine.

Finally, a similar argument may be applied to pyramidal  $C_{3v}$  trichlorides such as  $\text{PCl}_3$  where it may be shown that the chlorine-isotope pattern on the antisymmetric stretching mode should also show this characteristic pattern. The circumstances under which one would expect this are the same: *i.e.*, that the bending modes are well removed from the stretching modes, and that the  $A_1$  and  $E$  stretching modes are not too close. For most trichlorides the first qualification is usually fulfilled without difficulty, and it is interesting to explore just how close the  $A_1$  and  $E$  stretching modes have to be before this characteristic four-line pattern becomes significantly perturbed. This question may be answered by calculation or experimental observation, and it is interesting to note that King<sup>27</sup> found this isotope pattern on the  $E$  stretching mode of matrix-isolated  $\text{CHCl}_3$ , and the same pattern is seen to be present in the partially resolved spectrum of  $\text{SiCl}_3$  obtained by Jacox and Milligan.<sup>28</sup> In  $\text{PCl}_3$  itself, the  $A_1$  and  $E$  stretching modes lie at *ca.* 510 and *ca.* 490 respectively,<sup>29</sup> and the i.r. spectrum of the antisymmetric stretching region in  $\text{PCl}_3$  isolated in a nitrogen matrix (*ca.* 1 : 80 000) is shown in Figure 5(b). The characteristic chlorine isotope pattern is clearly visible even though the stretching modes are only *ca.* 20  $\text{cm}^{-1}$  apart. This simple model also yields an intensity ratio of *ca.* 5 : 1 for the  $E$  and

<sup>25</sup> E. B. Wilson, jun., J. C. Decius, and P. C. Cross, 'Molecular Vibrations,' McGraw-Hill, New York, 1955.

<sup>26</sup> J. H. Darling and J. S. Ogden, *J.C.S. Dalton*, 1972, 2496.

<sup>27</sup> S. T. King, *J. Chem. Phys.*, 1968, **49**, 1321.

<sup>28</sup> M. E. Jacox and D. E. Milligan, *J. Chem. Phys.*, 1968, **49**, 3130.

<sup>29</sup> See, for example, K. Nakamoto, 'Infrared spectra of Inorganic and Coordination Compounds,' Wiley-Interscience, New York, 1970.

$A_1$  stretching modes in  $\text{PCl}_3$ , and this is in satisfactory agreement with the observed spectrum.<sup>30</sup>

One might therefore anticipate that this pattern should be observed in a large number of  $C_{3v}$  or  $D_{3h}$  trichlorides, and that it might prove to be a diagnostic test for assigning the doubly degenerate stretching mode in these species. The extension of this analysis to other  $\text{MX}_3$  groupings (*e.g.*  $\text{MO}_3$  with  $^{18}\text{O}$  enrichment) is relatively straightforward, and

<sup>30</sup> S. N. Jenny, unpublished work.

matrix-isolation studies are ideally suited to achieving the high resolution necessary without the complications of rotational fine structure.

We thank the S.R.C. for support, Dr. C. G. Barraclough and Mr. D. Everett for many helpful discussions, and Dr. A. German and Miss I. Müller for the development work on superheater design.

[5/1581 Received, 11th August, 1975]